6-8-2023

Optical characterization of isothermal spin state switching in an Fe(II) spin crossover molecular and polymer ferroelectric bilayer

Saeed Yazdani

Kourtney Collier

Grace Yang

Jared Phillips

Ashley Dale

See next page for additional authors

Authors

Saeed Yazdani, Kourtney Collier, Grace Yang, Jared Phillips, Ashley Dale, Aaron Mosey, Samuel Grocki, Jian Zhang, Anne E. Shanahan, Ruihua Cheng, and Peter A. Dowben

PAPER • OPEN ACCESS

Optical characterization of isothermal spin state switching in an Fe(II) spin crossover molecular and polymer ferroelectric bilayer

To cite this article: Saeed Yazdani *et al* 2023 *J. Phys.: Condens. Matter* **35** 365401

View the article online for updates and enhancements.

Optical characterization of isothermal spin state switching in an Fe(II) spin crossover molecular and polymer ferroelectric bilayer

Saeed Yazdani[1] , **Kourtney Collier**[2] , **Grace Yang**[1], **Jared Phillips**[1] , **Ashley Dale**[1] ,
Aaron Mosey[1], **Samuel Grocki**[3], **Jian Zhang**[4] , **Anne E Shanahan**[5], **Ruihua Cheng**[1,*]
and Peter A Dowben[6,*]

[1] Department of Physics, Indiana University Purdue University Indianapolis (IUPUI), Indianapolis, IN
46202, United States of America
[2] Department of Mechanical and Energy Engineering, Purdue School of Engineering and Technology,
Indianapolis, IN 46202, United States of America
[3] Department of Chemistry, Purdue University, 575 W Stadium Ave, West Lafayette, IN 47907, United
States of America
[4] Molecular Foundry, Lawrence Berkeley National Laboratory, Berkeley, CA, United States of America
[5] Department of Chemistry and Chemical Biology, Indiana University Purdue University Indianapolis
(IUPUI), Indianapolis, IN 46202, United States of America
[6] Department of Physics and Astronomy, Jorgensen Hall, University of Nebraska, Lincoln, NE
68588-0299, United States of America

E-mail: rucheng@iupui.edu and pdowben1@unl.edu

Abstract

Using optical characterization, it is evident that the spin state of the spin crossover molecular complex [Fe{H_2B(pz)$_2$}$_2$(bipy)] (pz = tris(pyrazol-1-1y)-borohydride, bipy = 2,2′-bipyridine) depends on the electric polarization of the adjacent polymer ferroelectric polyvinylidene fluoride-hexafluoropropylene (PVDF-HFP) thin film. The role of the PVDF-HFP thin film is significant but complex. The UV–Vis spectroscopy measurements reveals that room temperature switching of the electronic structure of [Fe{H_2B(pz)$_2$}$_2$(bipy)] molecules in bilayers of PVDF-HFP/[Fe{H_2B(pz)$_2$}$_2$(bipy)] occurs as a function of ferroelectric polarization. The retention of voltage-controlled nonvolatile changes to the electronic structure in bilayers of PVDF-HFP/[Fe{H_2B(pz)$_2$}$_2$(bipy)] strongly depends on the thickness of the PVDF-HFP layer. The PVDF-HFP/[Fe{H_2B(pz)$_2$}$_2$(bipy)] interface may affect PVDF-HFP ferroelectric polarization retention in the thin film limit.

* Authors to whom any correspondence should be addressed.

(Some figures may appear in colour only in the online journal)

1. Introduction

Functional spin crossover (SCO) molecular complexes exhibiting a spin state transition that can be mediated by external stimulation such as light, temperature, electric field, and magnetic field [1–9], have significant potential for new molecular-based devices [4, 9–26]. In SCO molecular compounds, depending on the ligand field strength, the transition metal ion can adopt two different stable spin states called the low spin (LS) state and the high spin (HS) state and can be switched between these two states [1, 2, 8–10]. The transition from HS to LS state for many spin crossover complexes occurs away from temperatures. To implement these SCO molecular systems for device applications, it is crucial to modify their functionalities for use at room temperature. A ferroelectric layer, capable of changing the polarity of the electric polarization in the presence of an external electric field, facilitates switching spin states in SCO molecules at room temperature. Some SCO molecules such as $[Fe\{H_2B(pz)_2\}_2(bipy)]$ can be fabricated as a thin film via thermal evaporation under high-vacuum [14, 15, 27–32], as well as from solution. The transition temperature ($T_{1/2}$) and hysteresis of the spin state transition for $[Fe\{H_2B(pz)_2\}_2(bipy)]$ thin films can vary depending on film thickness [31], however, even the highest possible $T_{1/2}$ value is still far below room temperature, yet when combined with an organic ferroelectric, isothermal swicthing at room temperature can be made possible. A ferroelectric substrate may be utilized to facilitate the isothermal spin state switching of the deposited SCO molecular layer [11], as seen in figure 1, and variations of the polymer ferroelectric polyvinylidene fluoride (PVDF) have proven to be particularly effective [14, 15, 33, 34]. PVDF is a piezoelectric polymer with ferroelectric characteristics [35, 36]. Yet sensing the ferroelectric polarization in a memory circuit is challenging and thus combining a ferroelectric with an SCO complex provides a facile mechanism for sensing the ferroelectric polarization in a nonvolatile device [11, 14, 15] because of the dramatic conductivity changes that accompany the change in spin state, shown in figures 1(c) and (d). Indeed, the organic ferroelectric polyvinylidene fluoride-hexafluoropropylene (PVDF-HFP) also significantly affects the conductivity of spin crossover films as seen in figure 1. In this paper, the influence that PVDF-HFP film thickness and the polarity of ferroelectric polarization have on the spin state switching behavior of $[Fe\{H_2B(pz)_2\}_2(bipy)]$ at room temperature is investigated.

UV–Vis spectroscopy was employed here to study the temperature-dependent spin state switching of a single layer of $[Fe\{H_2B(pz)_2\}_2(bipy)]$ and the isothermal switching of bilayer samples of PVDF-HFP/$[Fe\{H_2B(pz)_2\}_2(bipy)]$ with different PVDF-HFP thicknesses. Switching to different spin
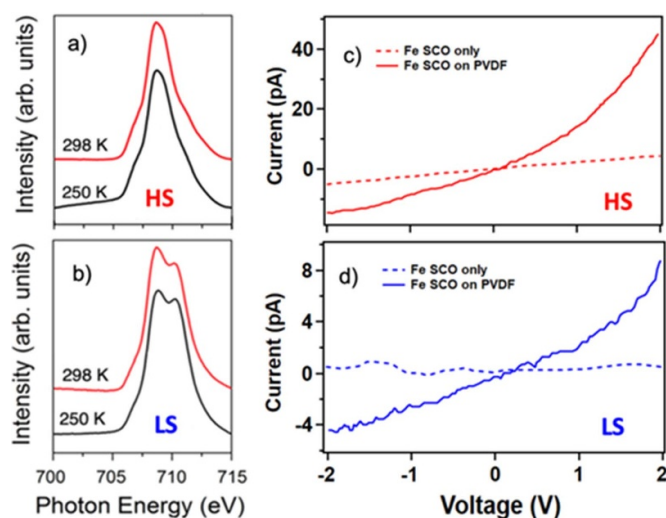

Figure 1. The changes in the x-ray absorption and conductivity for $[Fe\{H_2B(pz)_2\}_2(bipy)]$ film on PVDF-HFP, with the changing spin state. The synchrotron-based x-ray absorption (XAS) spectra of bilayer PVDF-HFP/ $[Fe\{H_2B(pz)_2\}_2(bipy)]$ bilayer samples for ferroelectric PVDF-HFP polarizations (a) up and (b) down, as discussed in detail elsewhere [14, 15]. The current–voltage conductance plots for $[Fe\{H_2B(pz)_2\}_2(bipy)]$ thin films and thin films on PVDF (c) in the high spin (HS) and (d) in low spin (LS) states [14, 15]. The transport measurements for HS and LS $[Fe\{H_2B(pz)_2\}_2(bipy)]$ thin films were taken at 298 K (red dashed line in (c)) and 150 K (the blue dashed line in (d)). The transport measurements at HS and LS for the $[Fe\{H_2B(pz)_2\}_2(bipy)]$ film on PVDF-HFP were taken at room temperature when the organic ferroelectric PVDF-HFP was polarized towards the $[Fe\{H_2B(pz)_2\}_2(bipy)]$ film (i.e. HS state denoted by the red solid line in (c)) and polarized away from the $[Fe\{H_2B(pz)_2\}_2(bipy)]$ film (i.e. LS state denoted by the blue solid line in (d)).

states can lead to a change in the optical absorption spectrum of $[Fe\{H_2B(pz)_2\}_2(bipy)]$ [37], the spin crossover complex studied here. The spin state switching of $[Fe(tBu_2qsal)_2]$ (FTBQS) has also been seen to lead to changes in optical absorption [38] and optical absorption has been applied to the study of other spin crossover complexes [39–43].

2. Materials and methods

The $[Fe\{H_2B(pz)_2\}_2(bipy)]$ molecules were synthesized as described in a previous article [44]. Samples for temperature-dependent SCO transition studies were 300 nm $[Fe\{H_2B(pz)_2\}_2(bipy)]$ thin films thermally evaporated on a glass substrate with an estimated growth rate of 0.2 nm s^{-1} under ultra high vacuum. Atomic force microscopy and a profilometer were utilized to calibrate the

growth rate and assess the film thickness ratios. The UV–Vis spectrometer used was Thermo Fisher Scientific G10S UV–Vis and the Fourier transform infrared (FTIR) spectrometer was a Thermo Fisher Scientific NICOLET iS10. A lab-built cryo-stage was used for low-temperature UV–Vis measurements. To study the effect of electric field on switching the spin state of [Fe{H$_2$B(pz)$_2$}$_2$(bipy)], bilayer PVDF-HFP/[Fe{H$_2$B(pz)$_2$}$_2$(bipy)] thin films with different thicknesses of PVDF-HFP were fabricated.

For bilayer samples, 10 nm of Ti was sputtered on the glass substrate to act as the bottom electrode. Various thicknesses of PVDF-HFP were deposited using the Langmuir–Blodgett (LB) technique. PVDF-HFP in solution was suspended in a water sub-phase for layer-by-layer LB deposition. A solution of 0.05% by weight of PVDF-HFP in acetone was made by mixing 40 mg PVDF-HFP with 100 ml acetone and then heating it to 90 °C until complete solvation was achieved. This solution was then added to de-ionized water and placed in the LB machine reservoir. For these parameters, each dip provides a thickness of around 0.7 nm. To achieve an optimal β phase in PVDF-HFP, thin films were annealed at different temperatures and characterized by FTIR spectroscopy. We found out that samples annealed for 3 h at 140 °C lead to a desirable β phase creation in the PVDF-HFP layer. Post-anneal, a 300 nm of [Fe{H$_2$B(pz)$_2$}$_2$(bipy)] film was added via thermal evaporation. A lab-built poling device with a removable top electrode was used to polarize the PVDF-HFP layer for bilayer samples. Depending on the desired polarity of the PVDF-HFP layer, a negative or positive voltage of 30 V was applied for 30 s then the bias voltage was gradually reduced back to zero. The UV–Vis measurements were done several times on multiple samples and similar results were acquired.

3. Optical characterization of the spin state change

A representative bond diagram of the [Fe{H$_2$B(pz)$_2$}$_2$(bipy)] molecule is shown in figure 2(a). The central Fe ion is bonded to nitrogen atoms from each of its ligands. N1 is the nitrogen of the bipyridine ligand while N2 and N3 correspond to the nitrogen atoms bonding the pyrazole ligands to the central Fe. The SCO transition for the [Fe{H$_2$B(pz)$_2$}$_2$(bipy)] molecular compound depends upon the changes in the bond length and ligand angular orientation within the molecule [31, 45]. When the molecule approaches the transition temperature, some bond lengths change, and the ligands rotate.

This bond length changes and ligand rotation occur mainly between the Fe ion and the bipyridine ligand (Fe-N1 ligand) [31, 44, 45]. A longer bond length means a weaker ligand interaction, which tends to favor the HS state with a total spin $S = 2$, while a shorter bond length corresponds to a stronger interaction, leading to the LS state with a total spin $S = 0$. Figure 2(b) compares the infrared spectra of [Fe{H$_2$B(pz)$_2$}$_2$(bipy)] in powder form with that of a thermally evaporated 300 nm thin film. A similar infrared
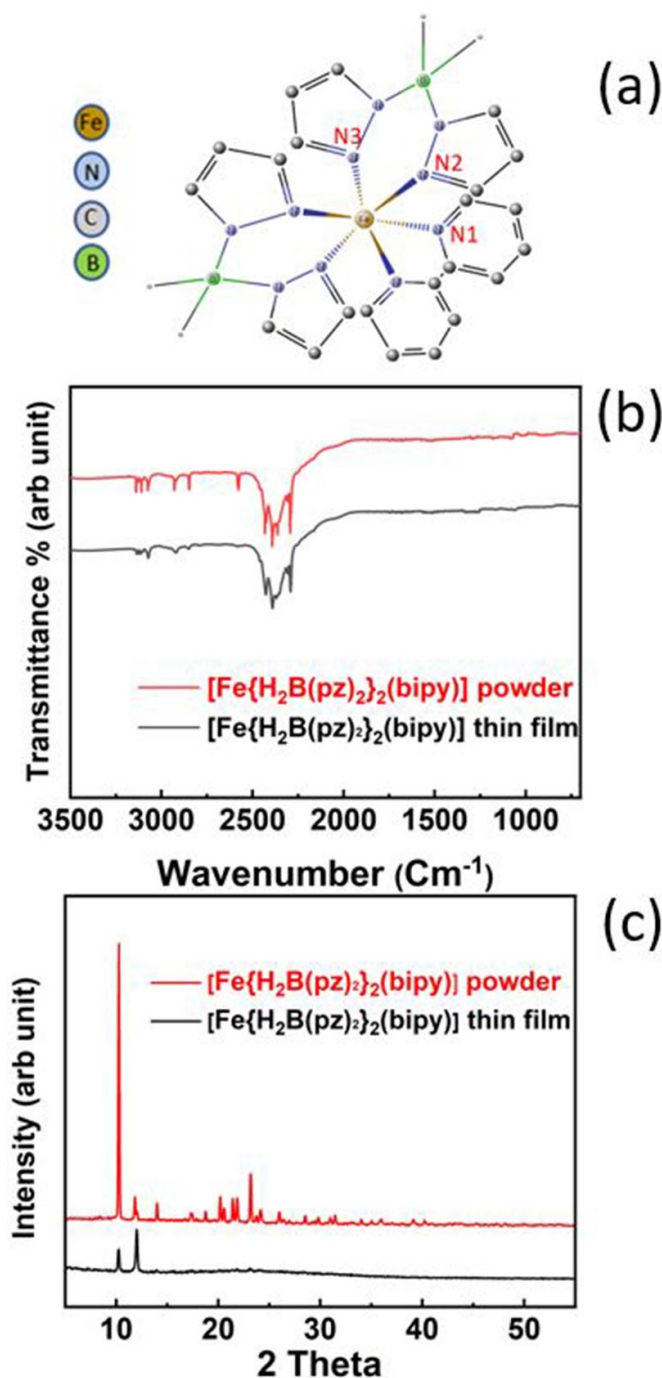
Figure 2. (a) The schematic diagram of the [Fe{H$_2$B(pz)$_2$}$_2$(bipy)] molecule. N1 is the nitrogen (blue) associated with the bipyridine ligand and N2 and N3 correspond to the nitrogen atoms in the pyrazole ligands. (b) The FTIR spectra of powder and 300 nm thin film [Fe{H$_2$B(pz)$_2$}$_2$(bipy)] molecules. (c) The XRD patterns of [Fe{H$_2$B(pz)$_2$}$_2$(bipy)] for powder and thin film samples respectively.

spectrum for both bulk and thin film indicates a successful thermal sublimation without decomposition. The existence of B-H vibrations in both powder and thin film spectra at 2416 cm^{-1} and 2277 cm^{-1}, and C-H vibrations

on 2841 cm^{-1}, 2911 cm^{-1}, and 3097 cm^{-1} verifies that [Fe{H$_2$B(pz)$_2$}$_2$(bipy)] molecules maintain integrity after evaporation. Observing no significant changes in the IR spectra of powder and the thin film implies that the [Fe{H$_2$B(pz)$_2$}$_2$(bipy)] is preserved after thin film fabrication and that similar thermal spin state transition properties are expected, as has been previously observed [32]. Additionally, x-ray diffraction (XRD) patterns shown in figure 2(c) confirm that the thin film sample preserves the [Fe{H$_2$B(pz)$_2$}$_2$(bipy)] structure however, the molecules of the thin film samples may have a preferential orientation on the substrate.

The spin transitions of the [Fe{H$_2$B(pz)$_2$}$_2$(bipy)] thin films stimulated by thermal effects were measured using UV–Vis spectroscopy. Comparing other methods for characterizing the spin state change, including x-ray absorption (XAS) and electric transport measurements, UV–Vis spectroscopy has some advantages as it avoids potential challenges due to high-energy x-ray or secondary electron-induced damage, voltage-induced charge trapping in electric transport measurements, or effects due to the different electronic structure at the surface of a molecular film [31].

An optimized film thickness is crucial for the optical absorption spectrum to become evident, and not perturbed by surface effects [31]. A 300 nm thick [Fe{H$_2$B(pz)$_2$}$_2$(bipy)] deposited film provides clear optical absorption spectra while the sample remains partially transparent, which is necessary for these UV–Vis measurements. The value in choosing a 300 nm thick [Fe{H$_2$B(pz)$_2$}$_2$(bipy)] deposited film is that in the optical studies of [Fe{H$_2$B(pz)$_2$}$_2$(bipy)] thin film adjacent to an organic ferroelectric (vide infra) the optical absorption of the [Fe{H$_2$B(pz)$_2$}$_2$(bipy)] thin film dominates over the much thinner ferroelectric layer. Furthermore, the spin state switching of a 300 nm thick [Fe{H$_2$B(pz)$_2$}$_2$(bipy)] film can be compared to prior efforts [31], where the transition in temperature has been investigated in detail. Figure 3(a) shows the temperature-dependent optical absorption spectra of a [Fe{H$_2$B(pz)$_2$}$_2$(bipy)] thin film with a thickness of 300 nm in a wide temperature range from room temperature to around 120 K. The spectra were normalized for a better quantitative comparison. The optical absorption spectra of [Fe{H$_2$B(pz)$_2$}$_2$(bipy)] molecules change with temperature and these changes are associated with a change in spin state.

In the HS state at room temperature, a weak absorption feature over a wide range of wavelengths with a crest of around 530 nm was observed. At the lower temperatures, spectral absorption intensity is dominated by broad absorption bands centered at 410 nm, and 570 nm, while the 640 nm band is much more intense at lower temperatures which correspond to the LS state. With decreasing temperature, these features in the UV–Vis spectra at around 410 nm, as well as 570 nm and 640 nm. These absorption features, representative of the low spin state, gain significant intensity at about 173 K to 148 K which is around the spin state transition temperature of 160 K, expected for evaporated thin films [32, 46–51]. As the sample temperature is reduced to 123 K, the LS state of [Fe{H$_2$B(pz)$_2$}$_2$(bipy)] dominates, as has been seen elsewhere using a number of other techniques [31, 32, 44–48].
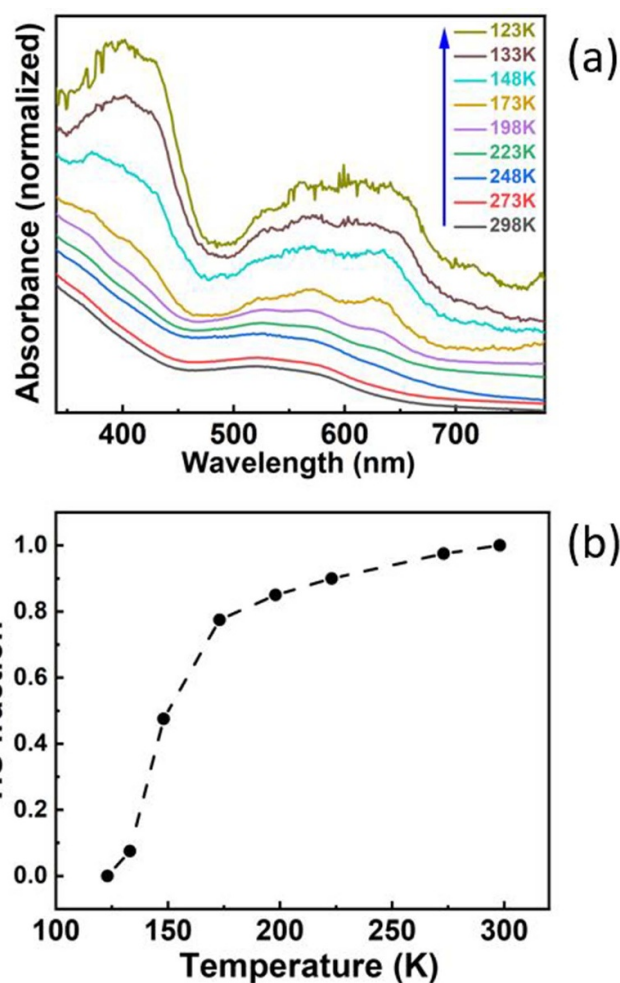
Figure 3. (a) The temperature-dependent UV–Vis spectra of a [Fe{H$_2$B(pz)$_2$}$_2$(bipy)] molecular thin film from room temperature to low temperatures and (b) the high spin (HS) state fraction of [Fe{H$_2$B(pz)$_2$}$_2$(bipy)] thin film, determined from the optical spectroscopy as a function of temperature.

The UV–Vis spectra of the same [Fe{H$_2$B(pz)$_2$}$_2$(bipy)] thin film show repeatable results when we ramp up the temperature back to room temperature, as shown in the supplementary file figure (S2), indicating the state switching process seen in optical spectroscopy results for [Fe{H$_2$B(pz)$_2$}$_2$(bipy)] is reversible. The thermal hysteresis seen in the optical studies here compares well with prior magnetic susceptibility results seen for a 300 nm thick [Fe{H$_2$B(pz)$_2$}$_2$(bipy)] deposited film [31]. These changes in the optical absorption are far more significant than observed for FTBQS which has also been seen to lead to similar changes in the optical absorption [38].

By analyzing the absorption spectra at the same wavelength and different temperatures, the HS fraction of the [Fe{H$_2$B(pz)$_2$}$_2$(bipy)] thin film at different temperatures was estimated. Figure 3(b) shows the fraction of molecules in the HS state for thin films of [Fe{H$_2$B(pz)$_2$}$_2$(bipy)] as a function of temperature. Temperature-dependent UV–Vis spectra provide a mechanism for the relative HS fraction at different temperatures to be calculated from the formula [37]:

$$\gamma_{HS}(T) = \frac{OD_\lambda(T \to 0)}{\Delta OD_\lambda} \left(1 - \frac{OD_\lambda(T)}{OD_\lambda(T \to 0)} \right)$$

where OD_λ is the optical density at $\lambda = 410$ nm, selected as the feature with the strongest temperature response in the spectra, and $\Delta OD_\lambda = OD_\lambda(T\to0) - OD_\lambda(T\to\infty)$, wherein the normalized data $OD_\lambda(T\to0)$ corresponds to the optical density of at the lowest temperature and $OD_\lambda(T\to\infty)$ is the optical density at the highest temperature. The calculated HS state fraction, with temperature, indicates a transition temperature, $(T_{1/2})$, from the HS state to the LS state occurring around 160 K. This spin state transition temperature is in agreement with other magnetic susceptibility measurements for [Fe(H$_2$B(pz)$_2$)$_2$(bipy)] [31, 32, 44–48], as well as Mössbauer spectroscopy and calorimetric measurements (where $T_{1/2} = 159.5$ K) [46].

4. Molecular ferroelectric film thickness dependence

Voltage-controlled nonvolatile switching of the [Fe{H$_2$B(pz)$_2$}$_2$(bipy)] electronic structure and spin state can be achieved well above the intrinsic thermal transition temperature by combining a [Fe{H$_2$B(pz)$_2$}$_2$(bipy)] thin film with an organic ferroelectric, like PVDF-HFP [11, 14, 15]. To explore this isothermal switching of the molecular bilayer further, we fabricated bilayer samples of PVDF-HFP/[Fe{H$_2$B(pz)$_2$}$_2$(bipy)] to facilitate the isothermal switching at room temperature, by altering the electric polarization polarity of the PVDF-HFP thin film. The interface of SCO molecules with a substrate can perturb the SCO functionality and spin state [9, 28, 29, 48–50], and the effect of an interface with a ferroelectric is particularly profound [14, 15, 33, 34, 52]. The PVDF-HFP thin films tend to be mostly in the nonpolar α phase when fabricated at room temperature, whereas the β phase is desirable due to its high electric polarization. There are several approaches to achieving a dominant ferroelectric β phase in PVDF. One method is to use additives such as hydrated ionic salts, clay, PMMA, ZnO, TiO$_2$, and graphene [53, 54]. In our case, however, a thermal treatment method of the molecular ferroelectric thin film was preferred. It has been shown and repeatedly confirmed that thermal annealing is an effective approach to forming the ferroelectric β phase crystalline ordering in PVDF-HFP thin films [55–58].

While for thicker PVDF molecular films, in the range of microns, XRD is a powerful tool for characterizing the crystalline structure, for PVDF-HFP thin films with a thickness in the range of nanometer, XRD provides a very weak signal. As here in these studies we are investigating much thinner films, our approach to the characterization of the different crystalline phases of the PVDF-HFP thin films was to use FTIR spectroscopy. The IR bands at 841 cm^{-1} and 879 cm^{-1} correspond to the β phase. Before annealing a PVDF-HFP thin film, only a very weak signal of β-phase is detected, based on the data shown in figure 4. The thermal optimization was undertaken with a series of 150 layer thick PVDF-HFP samples.
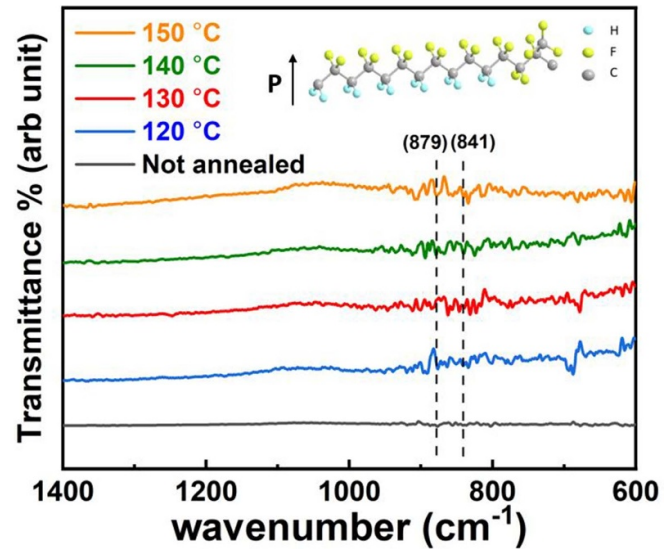

Figure 4. The FTIR spectra of 150 layer thick PVDF-HFP thin films annealed at argon atmosphere for 180 min. A schematic diagram of PVDF-HFP in the β phase is shown in the inset.

These were annealed at different temperatures (from 120 °C to 150 °C) for 180 min in an argon gas atmosphere to better optimize the crystal structure of the PVDF-HFP thin films, as seen in the IR spectra of figure 4. The IR signature of the PVDF-HFP β-phase improves with annealing, as indicated by the increase in the β-phase IR features. Clearly, annealing significantly improves the β-phase of the PVDF-HFP thin films. Decreasing the ferroelectric thin film thickness will decrease the coercive voltage [11, 36], but there must be polarization retention in the ferroelectric layer for nonvolatile molecular device applications [11]. To study the effect of PVDF-HFP polarization and thickness on isothermal switching of [Fe{H$_2$B(pz)$_2$}$_2$(bipy)] thin films, a series of samples with different layers of PVDF-HFP, ranging from 5 to 25 layers, with a constant thickness (300 nm) of the [Fe{H$_2$B(pz)$_2$}$_2$(bipy)] layer were prepared.

The voltage can be applied to the molecular bilayer structure in the capacitive geometry, as indicated in figures 5(a) and (b). Figure 6(a) shows the UV–Vis spectra of the bilayer sample with 5 layers of PVDF-HFP after applying opposite electric fields at room temperature. These optical measurements show that for the sample with 5 layers of PVDF-HFP, isothermal voltage-controlled switching between the [Fe{H$_2$B(pz)$_2$}$_2$(bipy)] spin states does not occur by changing the applied electric field polarity to the adjacent PVDF-HFP thin film. Either the voltage applied was not high enough to overcome the coercive force of the PVDF-HFP layer, so the polarization was not altered, or the polarization prefers one direction (i.e. up) and polarization in the opposite direction (down) is not retained and quickly reverts to the favored polarization direction.

This lack of polarization retention is a common problem with ferroelectric thin films, in the thin film limit [59, 60]. In the absence of polarization retention, an 'up' ferroelectric
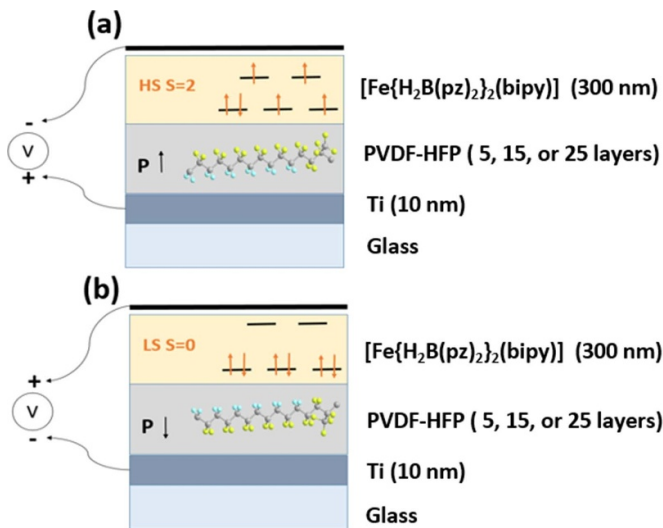
Figure 5. A schematic cross-section diagram of the bilayer the PVDF-HFP/[Fe{H$_2$B(pz)$_2$}$_2$(bipy)] studied, with the polarization of PVDF-HFP thin film toward a specific direction, can cause the upper SCO layer to switch to the (a) high spin (HS) when the PVDF-HFP layer was polarized upward or (b) the low spin (LS) states when the PVDF_HFP layer was polarized to the downward, schematically indicated.

polarization is expected here [61]. The likely problem here is the polarization retention because the applied electric field should nominally lead to the reversal of the PVDF-HFP ferroelectric polarization since the applied voltage is much larger than the PVDF-HFP coercive voltage for this film thickness [36] and the coercive voltage scales with film thickness [11, 36]. Furthermore, this voltage does affect the bilayers with thick PVDF-HFP film thicknesses, where retention is more likely and the barrier to spontaneous ferroelectric polarization reversal is higher.

By increasing the thickness of PVDF-HFP thin films to 15 layers, the spectra taken after applying opposite applied electric fields to the ferroelectric layer start showing a slight difference as seen in figure 6(b). In terms of changing the spin state of the [Fe{H$_2$B(pz)$_2$}$_2$(bipy)] in the PVDF-HFP/[Fe{H$_2$B(pz)$_2$}$_2$(bipy)] bilayer structure, the best result was achieved for the sample fabricated with 25 layers of PVDF-HFP (figure 6(c)). Reversible voltage-controlled switching from both the HS and the LS states of [Fe{H$_2$B(pz)$_2$}$_2$(bipy)] was observed and associated with the changing polarity of the PVDF-HFP thin films. By polarizing the PVDF-HFP upwards, the [Fe{H$_2$B(pz)$_2$}$_2$(bipy)] HS optical absorption peak at 530 nm associated with the HS state was observed. On the other hand, [Fe{H$_2$B(pz)$_2$}$_2$(bipy)] molecules successfully switched to the LS state when the PVDF-HFP layers were polarized downward, based on the optical spectra of figure 6(c). These results agree with previous experiments, where the spin state and consequently the conductivity of [Fe{H$_2$B(pz)$_2$}$_2$(bipy)] molecules changed by altering the electric polarization direction of the adjacent PVDF-HFP thin films [14, 15]. In other words, a too thin layer of PVDF-HFP causes the [Fe{H$_2$B(pz)$_2$}$_2$(bipy)] molecules
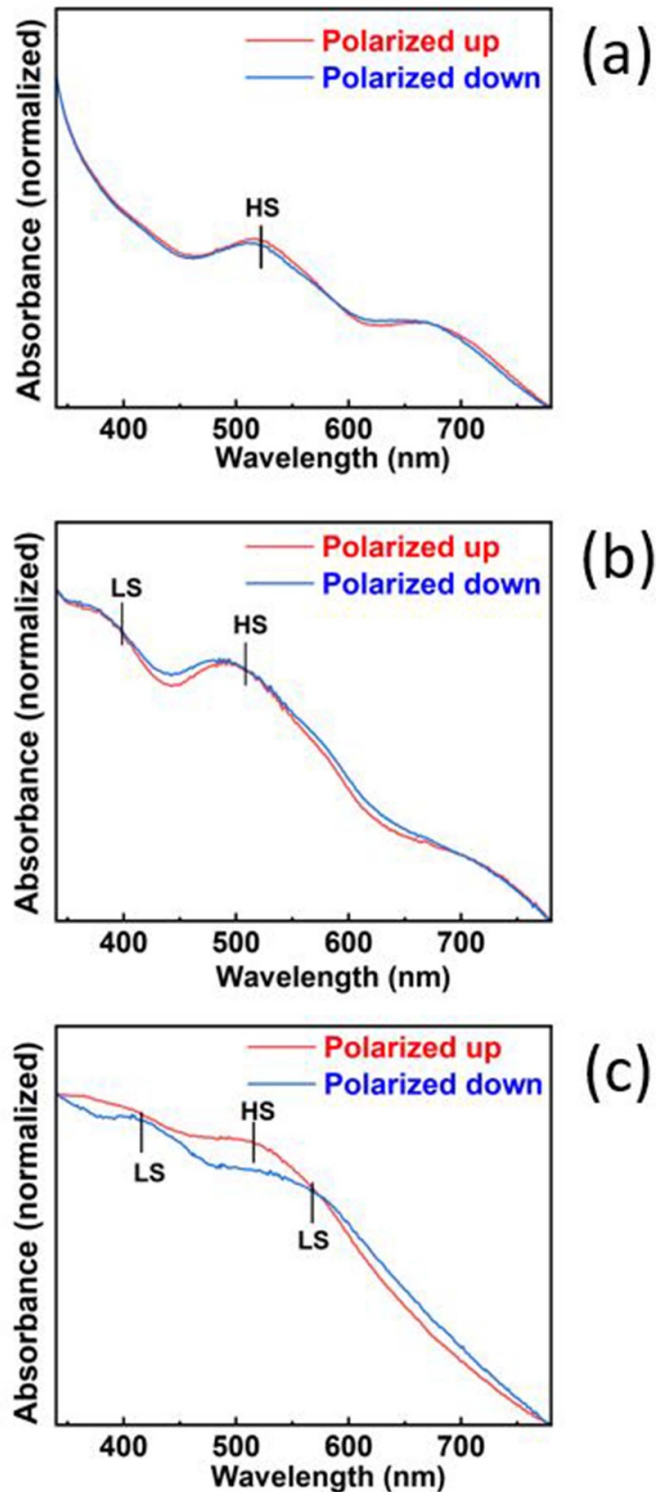
Figure 6. The room temperature UV–Vis spectra of the bilayer samples were made with (a) 5 layers (b) 15 layers and (c) 25 layers of PVDF-HFP substrates polarized toward different directions.

to become locked in the HS state due to the lack of ferroelectric polarization retention resulting tendency in an 'up' ferroelectric polarization [61] where the HS is dominant in the adjacent [Fe{H$_2$B(pz)$_2$}$_2$(bipy)] layer [15, 52]. Although

for thicker organic ferroelectric films the coercive force is larger [35, 36], there is polarization retention, and changing the ferroelectric polarization leads to clear changes in the optical spectra reflecting the change in the spin state of the adjacent [Fe{H$_2$B(pz)$_2$}$_2$(bipy)] layer. Changing in the ferroelectric polarization in the thicker PVDF-HFP layer does not, however, lead to complete isothermal voltage-controlled switching between the HS and LS states in the adjacent [Fe{H$_2$B(pz)$_2$}$_2$(bipy)] layer. Comparing the optical spectra results for the bilayer PVDF-HFP/[Fe{H$_2$B(pz)$_2$}$_2$(bipy)] with the temperature-dependent measurement of single layer [Fe{H$_2$B(pz)$_2$}$_2$(bipy)] molecular thin film, a smaller portion of [Fe{H$_2$B(pz)$_2$}$_2$(bipy)] molecules switch isothermally by altering the ferroelectric polarization of the adjacent PVDF-HFP thin film. From figure 6(c), it is estimated that for the sample made by 25 layers of PVDF-HFP, around half (53%–57%) of the adjacent [Fe{H$_2$B(pz)$_2$}$_2$(bipy)] switched isothermally to the LS spin when the PVDF-HFP was polarized downward. This incomplete switching can be due to [Fe{H$_2$B(pz)$_2$}$_2$(bipy)] film thickness. It is estimated that for 1 to about 20–24 molecular layers of [Fe{H$_2$B(pz)$_2$}$_2$(bipy)], interface effects lead to nearly complete spin state switching [52], but for 60–75 molecular layers (65 nm) of [Fe{H$_2$B(pz)$_2$}$_2$(bipy)], the spin state switching in the [Fe{H$_2$B(pz)$_2$}$_2$(bipy)] due to polarization reversal in the adjacent PVDF-HFP layer is incomplete [14]. Here we have a 300 nm thick film of [Fe{H$_2$B(pz)$_2$}$_2$(bipy)] and can safely surmise that the spin state switching mediated by the adjacent molecular ferroelectric layer mostly occurs in the molecular layers closer to the interface with the PVDF-HFP.

Polarization retention in PVDF copolymer films has been observed in films as thin as 1 nm, indeed in films as thin as 2 molecular layers [36]. The fact that polarization retention is not seen in the thinnest films studied here indicates that not only does the PVDF-HFP affect and influence the adjacent [Fe{H$_2$B(pz)$_2$}$_2$(bipy)] layer, as discussed at the outset, but that [Fe{H$_2$B(pz)$_2$}$_2$(bipy)] layer has an influence of the PVDF-HFP.

5. Conclusion

In this paper, we have demonstrated that optical spectroscopy can be used to study the switching of spin states in the [Fe{H$_2$B(pz)$_2$}$_2$(bipy)] molecular thin film, as has been seen for other spin crossover molecular systems [42]. Temperature-dependent UV–Vis measurements confirmed that the transition temperature, $T_{1/2}$, of the [Fe{H$_2$B(pz)$_2$}$_2$(bipy)] SCO molecular thin film from the HS to LS spin state occurs at around 160 K, consistent with prior studies [31, 32, 44–48]. FTIR spectroscopy of PVDF-HFP revealed that post-annealing treatments improve the β phase for ferroelectric PVDF-HFP thin films. A thin film of PVDF-HFP in the β phase allows isothermal switching of the spin state of an adjacent [Fe{H$_2$B(pz)$_2$}$_2$(bipy)] thin films at room temperature to occur. Yet polarization retention is a problem in ferroelectric PVDF-HFP/[Fe{H$_2$B(pz)$_2$}$_2$(bipy)] bilayers, so choosing the correct thickness of PVDF-HFP

is crucial. Our experiment indicates that switching different spin states of [Fe{H$_2$B(pz)$_2$}$_2$(bipy)] molecules, in a PVDF-HFP/[Fe{H$_2$B(pz)$_2$}$_2$(bipy)] bilayer structure, is possible with 25 layers of PVDF-HFP which corresponds to a thickness of around 20 nm. When the PVDF-HFP ferroelectric is too thin, an absence of polarization retention appears for the bilayer PVDF-HFP/[Fe{H$_2$B(pz)$_2$}$_2$(bipy)]. This is of profound important for device applications as if there is a limit to the ferroelectric layer thickness in the PVDF-HFP/[Fe{H$_2$B(pz)$_2$}$_2$(bipy)] bilayer, then there is a limit to the reduction of the coercive voltage for non-volatile switching. Other suitable organic ferroelectrics may need to be investigated, but clearly, the influence of the organic ferroelectric PVDF-HFP on the adjacent spin crossover [Fe{H$_2$B(pz)$_2$}$_2$(bipy)] thin film in the bilayer structure is more than simply aiding in the deterministic switching of the spin state.

Data availability statement

All data that support the findings of this study are included within the article (and any supplementary files).

Conflict of interest

There are no conflicts to declare.

ORCID iDs

Saeed Yazdani ● https://orcid.org/0000-0001-7691-1466
Kourtney Collier ● https://orcid.org/0000-0002-6529-5001
Jared Phillips ● https://orcid.org/0000-0001-6914-0560
Ashley Dale ● https://orcid.org/0000-0001-8233-5258
Jian Zhang ● https://orcid.org/0000-0003-0274-0814
Ruihua Cheng ● https://orcid.org/0000-0003-1579-8097
Peter A Dowben ● https://orcid.org/0000-0002-2198-4710

References

[1] Halcrow M A 2013 *Chem. Commun.* **49** 10890–2
[2] Collet E and Guionneau P 2018 *C. R. Chim.* **21** 1133–51
[3] Thakur S *et al* 2021 *J. Phys. Chem.* C **125** 13925–32
[4] Mahfoud T, Molnár G, Bonhommeau S, Cobo S, Salmon L, Demont P, Tokoro H, Ohkoshi S I, Boukheddaden K and Bousseksou A 2009 *J. Am. Chem. Soc.* **131** 15049–54
[5] Ridier K, Nicolazzi W, Salmon L, Molnár G and Bousseksou A 2022 *Adv. Mater.* **34** 2105468
[6] Xie K P, Ruan Z Y, Chen X X, Yang J, Wu S G, Ni Z P and Tong M L 2022 *Inorg. Chem. Front.* **9** 1770–6

[7] Terrero R, Avila Y, Mojica R, Cano A, Gonzalez M, Avila M and Reguera E 2022 *New J. Chem.* **46** 9618–28

[8] Gütlich P and Goodwin H A (eds) 2004 Topics in current chemistry *Spin Crossover in Transition Metal Compounds* vol 1 (Berlin: Springer) (https://doi.org/10.1007/b83735)

[9] Kumar K S and Ruben M 2021 Sublimable spin-crossover complexes *Angew. Chem., Int. Ed.* **29** 7502–21

[10] Gütlich P, Garcia Y and Goodwin H A 2000 *Chem. Soc. Rev.* **29** 419–27

[11] Ekanayaka T K *et al* 2021 *Magnetochemistry* **7** 37

[12] Molnár G, Salmon L, Nicolazzi W, Terki F and Bousseksou A 2014 *J. Mater. Chem. C* **2** 1360

[13] Tissot A, Kesse X, Giannopoulou S, Stenger I, Binet L, Rivière E and Serre C 2019 *Chem. Commun.* **55** 194–7

[14] Mosey A, Dale A S, Hao G, N'Diaye A, Dowben P A and Cheng R 2020 *J. Phys. Chem. Lett.* **11** 8231–7

[15] Hao G *et al* 2019 *Appl. Phys. Lett.* **114** 032901

[16] Kahn O and Martinez C J 1998 Spin-transition polymers *Science* **279** 44–48

[17] Bousseksou A, Molnár G, Salmon L and Nicolazzi W 2011 *Chem. Soc. Rev.* **40** 3313–35

[18] Bousseksou A, Molnár G, Demont P and Menegotto J 2003 *J. Mater. Chem.* **13** 2069–71

[19] Molnár G, Rat S, Salmon L, Nicolazzi W and Bousseksou A 2018 *Adv. Mater.* **30** 1703862

[20] Rotaru A, Dugay J, Tan R P, Guralskiy I A, Salmon L, Demont P, Carrey J, Molnár G, Respaud M and Bousseksou A 2013 *Adv. Mater.* **25** 745–9

[21] Lefter C, Davesne V, Salmon L, Molnár G, Demont P, Rotaru A and Bousseksou A 2016 *Magnetochemistry* **11** 18

[22] Lefter C, Tan R, Dugay J, Tricard S, Molnár G, Salmon L, Carrey J, Nicolazzi W, Rotaru A and Bousseksou A 2016 *Chem. Phys. Lett.* **16** 138–41

[23] Mahfoud T, Molnár G, Cobo S, Salmon L, Thibault C, Vieu C, Demont P and Bousseksou A 2011 *Appl. Phys. Lett.* **99** 053307

[24] Hao G, Cheng R and Dowben P A 2020 *J. Phys.: Condens. Matter* **32** 234002

[25] Khusniyarov M M 2016 *Chem. Eur. J.* **17** 15178–91

[26] Kumar K S and Ruben M 2017 *Coord. Chem. Rev.* **1** 176–205

[27] Hao G *et al* 2021 *Magnetochemistry* **2** 135

[28] Beniwal S *et al* 2016 *J. Phys.: Condens. Matter* **28** 206002

[29] Zhang X, Zhang X, Zhang X, Yin Y, Xu X and Dowben P A 2018 *Chem. Commun.* **54** 944–7

[30] Kumar K S, Studniarek M, Heinrich B, Arabski J, Schmerber G, Bowen M, Boukari S, Beaurepaire E, Dreiser J and Ruben M 2018 *Adv. Mater.* **30** 1705416

[31] Jiang X *et al* 2019 *J. Phys.: Condens. Matter* **31** 315401

[32] Zhang X, Palamarciuc T, Rosa P, Létard J F, Doudin B, Zhang Z, Wang J and Dowben P A 2012 *J. Phys. Chem. C* **116** 23291–6

[33] Wäckerlin C, Donati F, Singha A, Baltic R, Decurtins S, Liu S X, Rusponi S and Dreiser J 2018 *J. Phys. Chem. C* **122** 8202–8

[34] Angulo-Cervera J E, Piedrahita-Bello M, Mathieu F, Leichle T, Nicu L, Salmon L, Molnár G and Bousseksou A 2021 *Magnetochemistry* **7** 114

[35] Lovinger A J 1982 Poly(Vinylidene Fluoride) *Developments in Crystalline Polymers—1* The Developments Series ed D C Bassett vol 33 (Dordrecht: Springer) pp 196–273

[36] Blinov L M, Fridkin V M, Palto S P, Bune A V, Dowben P A and Ducharme S 2000 *Phys.-Usp.* **43** 243

[37] Naggert H, Bannwarth A, Chemnitz S, von Hofe T, Quandt E and Tuczek F 2011 *Dalton Trans.* **40** 6364–6

[38] Koptur-Palenchar J, Gakiya-Teruya M, Le D, Jiang J, Zhang R, Jiang X, Cheng H P, Rahman T S, Shatruk M and Zhang X X 2022 *npj 2D Mater. Appl.* **6** 59

[39] Hauser A 2004 Light-induced spin crossover and the high-spin→low-spin relaxation *Spin Crossover in Transition Metal Compounds II* ed P Gütlich and H A Goodwin Topics in Current Chemistry vol 234 (Berlin: Springer) pp 155–98

[40] Chakraborty P, Enachescu C, Walder C, Bronisz R and Hauser A 2012 *Inorg. Chem.* **51** 9714–22

[41] Phan H V *et al* 2012 *Chem. Eur. J.* **18** 15805–15

[42] Chergui M and Collet E 2017 *Chem. Rev.* **117** 11025–65

[43] Ridier K *et al* 2019 *Adv. Mater.* **31** 1901361

[44] Palamarciuc T, Oberg J C, El Hallak F, Hirjibehedin C F, Serri M, Heutz S, Létard J F and Rosa P 2012 *J. Mater. Chem.* **22** 9690–5

[45] Real J A, Muñoz M C, Faus J and Solans X 1997 *Inorg. Chem.* **36** 3008–13

[46] Moliner N *et al* 2002 *J. Phys. Chem. B* **106** 4276–83

[47] Pronschinske A, Bruce R C, Lewis G, Chen Y, Calzolari A, Buongiorno-Nardelli M, Shultz D A, You W and Dougherty D B 2013 *Chem. Commun.* **49** 10446–52

[48] Zhang X *et al* 2015 *J. Phys. Chem. C* **119** 16293–302

[49] Gruber M and Berndt R 2020 *Magnetochemistry* **6** 35

[50] Yazdani S, Phillips J, Ekanayaka T K, Dowben P and Cheng R 2023 *Molecules* **28** 3735

[51] Zhang X *et al* 2017 *Adv. Mater.* **29** 1702257

[52] Zhang X, Palamarciuc T, Létard J F, Rosa P, Lozada E V, Torres F, Rosa L G, Doudin B and Dowben P A 2014 *Chem. Commun.* **50** 2255–7

[53] Zhang X, Lang W Z, Xu H P, Yan X, Guo Y J and Chu L F 2014 *J. Memb. Sci.* **1** 458–70

[54] Mokhtari F, Shamshirsaz M, Latifi M and Asadi S 2017 *J. Text. Inst.* **108** 906–14

[55] Mahdavi Varposhti A, Yousefzadeh M, Kowsari E and Latifi M 2020 *Macromol. Mater. Eng.* **305** 1900796

[56] Park J H, Kurra N, AlMadhoun M N, Odeh I N and Alshareef H N 2015 *J. Mater. Chem. C* **3** 2366–70

[57] Kaur S, Kumar A, Sharma A L and Singh D P 2017 *J. Mater. Sci.* **28** 8391–6

[58] Satthiyaraju M and Ramesh T 2019 *Mater. Res. Express* **6** 105366

[59] Scott J F, Araujo C A, Meadows H B, McMillan L D and Shawabkeh A 1989 *J. Appl. Phys.* **66** 1444–53

[60] Gao P *et al* 2012 *Adv. Mater.* **24** 1106–10

[61] Duan C G, Sabiryanov R F, Liu J, Mei W N, Dowben P A and Hardy J R 2005 *J. Appl. Phys.* **97** 10A915